

# Real-Time Optimization and Stabilization of Distributed Parameter Systems with Piezoelectric Elements.

Karl-Heinz Hoffmann and Nikolai D. Botkin

Stiftung *c a e s a r*, Center of Advanced European Studies and Research, Bonn, Germany

**Abstract** The investigation of this paper is related to the design of active real-time controls which provide the desired performance of flexible constructions subjected to varying disturbances. Physical controllers are piezoelectric elements that transform applied voltages into mechanical forces and moments. Control voltages are computed on the base of signals measured on piezoelectric sensors. The underlying structure is a thin plate or shell. The piezoelectric elements are either surface mounted or embedded within the structure. Conventional averaging procedures are used to eliminate the thickness in mathematical models. A homogenization procedure is used to reduce structures with large number of piezoelectric elements to the case of continuously distributed input or output signals.

## 1 CONCEPTION OF ACTIVE CONTROL

The idea of active real-time control is intensively developed during several last years. The acute interest to this method of elimination of parasitic disturbances is caused by the rapid development of the material science, electronics, and computer technology. This approach can be characterized as an intelligent one by contrast with routine approaches based on the reenforcement of the construction, which makes it heavier and more expensive.

Consider a precise structure subjected to varying acoustic or thermal conditions. Even though carefully designed, it will be disturbed as a result of unpredictable thermal gradients or acoustic pressures. One way to prevent this is to build the structure from massive components and to provide very good isolation from external influences. An alternative way is to use a set of actuators and sensors connected by a feedback loop. In this case, we exploit the main virtue of the feedback which is to attenuate the effect of disturbances within the bandwidth of the control system. Active structures may be cheaper or lighter than passive structures with comparable performances, or they can sufficiently improve the performance. Here, we want to refer to the following classical example (see [1]). The telescope at ESO in La Silla, Chili, uses adaptive optics for the compensation of atmospheric turbulences. The primary mirror of the telescope is connected at the back to a set of hundred actuators. The control system uses an image analyzer to evaluate the distributed amplitude of the perturbation. The correction is computed to minimize the effect of the perturbation and is applied to the actuators. The computation of the correcting forces is based on the influence matrix describing the relation between the actuator forces and the wave front changes. This matrix is determined experimentally

from the analysis of images. Note that such a relatively simple relation between the controls and objectives is not always possible. Very often, this relation is described by a very complicated mathematical model based on nonlinear partial differential equations. This approach is carefully developed in the monograph [2]. The schema of the active control design is shown on Figure 1. We study the real-time control design with the use of piezoelectric elements as actuators and sensors. Piezoelectric materials exhibit significant deformations in response to an applied electric field as well as produce polarization in response to mechanical strains.

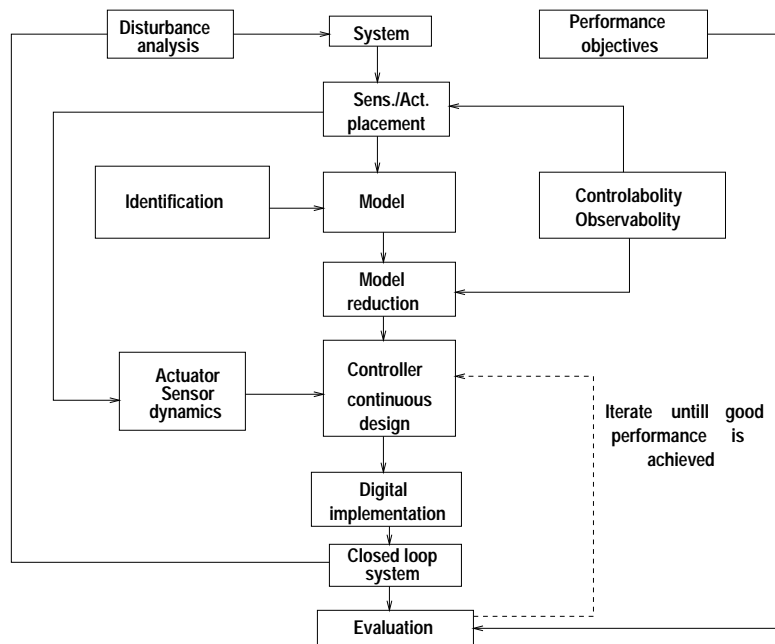


**Figure 1.** Steps of the control design

The field-strain relations are nearly linear for small electric fields and deformations, which is an advantage when employing piezoelectric elements in control systems. The linear direct and converse constitutive relationships for piezoelectric materials (see, e.g., [3] and compare with [4] concerning more general models) are given by

$$\begin{aligned}\sigma_{ij} &= C_{ijkl}\varepsilon_{kl} - e_{kij}E_k, \\ D_i &= \varepsilon_{ij}E_j + e_{ikl}d_{kl}.\end{aligned}\tag{1}$$

Here,  $D$  and  $E$  denote the electric displacement and field, respectively, while  $\epsilon$ ,  $\mathcal{E}$ , and  $C$  denote the material dielectric tensor, the stress piezoelectric tensor and the elastic stiffness tensor, respectively. As usually, the repeated subscripts indicate summation; Latin subscripts run from 1 to 3 whereas Greek subscripts run from 1 to 2. To cover all possible cases of piezoelectric materials, assume that all coefficients may be nonzero and different. This is really the case for the triclinic crystal systems (see [3]).

Note that relations (1) are nonlinear with respect to the displacements  $u_i = y_i(x_1, x_2, x_3, t) - x_i$ ,  $i = 1, 2, 3$ , because the strain tensor contains quadratic terms, namely

$$\epsilon_{ij} = \frac{1}{2} \left( \frac{\partial u_i}{\partial x_j} + \frac{\partial u_j}{\partial x_i} + \frac{\partial u_k}{\partial x_i} \cdot \frac{\partial u_k}{\partial x_j} \right), \quad i, j = 1, 2, 3. \quad (2)$$

Therefore, the energy density of a piezoelectric medium,

$$\chi = \frac{1}{2} (\sigma_{ij} \epsilon_{ij} - E_i D_i), \quad (3)$$

is not quadratic and may be not convex, which may violate the uniqueness of solutions.

The underlying structure is a plate or shell in our case. The piezoelectric elements are either surface mounted or embedded within the structure. Therefore, we have to describe the coupling between two media with different elastic, electric and piezoelectric properties. Then, we have to apply an averaging to exclude the thickness and obtain a thin composite structure. Moreover, the interaction between the piezoelectric elements and the substrate is time-dependent with various transient effects; hence dynamic models are necessary.

We derive our models using the following variational principle: the work of inertia forces plus the variation of the free energy must be equal to the work of external forces. The free energy is the sum of the free energies of the piezoelectric elements and the substrate. One advantage of this approach is that the right interface conditions are being obtained automatically.

The design of a control law must be done in accordance with that the actuators and sensors yield unbounded input and output operators in the mathematical problem formulation. An extension of  $H^\infty$  theory (see [5]) to this case is developed in [6]. A way to avoid unbounded input and output operators is related to the homogenization of model equations. If the number of actuators and sensors is large enough, we can assume that it goes to infinity, whereas the size of each element tends to zero. Some special procedure based on two-scale convergence is applied to the model equations in order to obtain limiting equations. It is remarkable that the limiting equations are much better than the original ones: they do not contain unbounded operators and discontinuous coefficients because the interface is smeared when applying the homogenization. Numerical simulations prove that the control law designed using the limiting equations provides some good performance of the original controlled system; the number of actuators does not have to be too large: 30-40 elements are sufficient to provide some good consistence.

Summarizing, we can outline the frameworks of our study as follows:

- Derivation of mathematical models of thin plates and shells with actuators and sensors in various configurations.
- Mathematical investigation of the model equations concerning their solubility and correctness including nonlinear cases.
- Estimation of unknown parameters.
- Homogenization.
- Feedback control design using  $H^\infty$  theory or the theory of differential games.

## 2 MATHEMATICAL MODELS OF THIN PLATES AND SHELLS WITH SURFACE MOUNTED PIEZOELECTRIC ELEMENTS

### 2.1 Variational Principle

We use a variational principle (see [7]) for the derivation of dynamic equations:

$$\text{The work of the inertia forces } + \delta F = 0, \quad (4)$$

where  $\delta F$  is the variation of the total free energy. The total free energy  $F$  can be computed through the densities of the free energy for the substrate, piezoelectric material and surrounding substance (say air). Thus,

$$F = \int_{V_S} \mathcal{F}_S + \int_{V_P} \mathcal{F}_P + \int_{V_A} \mathcal{F}_A. \quad (5)$$

Here,  $\mathcal{F}_P$ ,  $\mathcal{F}_S$  and  $\mathcal{F}_A$  are the densities of the free energy;  $V_P$ ,  $V_S$  and  $V_A$  are the corresponding volumes. Note that each of volumes  $V_P$ ,  $V_S$  and  $V_A$  can be divided into several parts to simplify the computation of the free energy or to account the discontinuity of material parameters that appear due to a multi piece structure of the system.

### 2.2 Elimination of the Thickness

To obtain two-dimensional structures, we have to average along the thickness. This can be achieved using the Kirchhoff-Love-Koiter hypothesis that allow us to express all components of the strain tensor through the displacement of points lying on some reference surface (say middle surface). An expansion of the electric field with respect to the deviation from the reference surface is also necessary.

Let  $Q$  be a point of the plate,  $M$  orthogonal projection of  $Q$  onto the middle surface,  $u_1, u_2$  longitudinal displacements of  $M$  and  $w$  the transversal displacement of  $M$ . According to the Kirchhoff-Love-Koiter hypothesis (see, e.g., [8]), the components of the strain tensor at the point  $Q$  are given by

$$\begin{aligned} \varepsilon_{\alpha\beta} &= 1/2(u_{\alpha x_\beta} + u_{\beta x_\alpha} + w_{x_\alpha} w_{x_\beta}) - x_3 \cdot w_{x_\alpha x_\beta}, \\ \varepsilon_{3\alpha} &= \varepsilon_{\alpha 3} = 0, \quad \varepsilon_{33} \text{ is found from } \sigma_{33} = 0. \end{aligned} \quad (6)$$

The assumption  $\varepsilon_{3\alpha} = \varepsilon_{\alpha 3} = 0$ ,  $\alpha = 1, 2$ , means the absence of transverse shear strains, which implies the conservation of the normal. The component  $\varepsilon_{33}$  is found

from the hypothesis of plain stresses. Therefore,  $\varepsilon_{33}$  is material and field dependent. The first approximation of the electric field within a thin piezoelectric element whose longitudinal faces are covered by a metal is given by

$$E_1 = E_2 = 0, \quad E_3 = V/h, \tag{7}$$

where  $V$  is a voltage applied between the longitudinal faces, and  $h$  is the thickness of the piezoelectric element. Now we are in position to compute the total free energy and exclude the thickness using (3), (5), (6) and (7). The application of (4) yields dynamic equations. Note that the Kirchhoff-Love-Koiter hypotheses can be replaced by more complex assumptions permitting transverse shear strains. This demands two additional variables describing the change of the normal. Some more accurate approximation of the electric field can be archived through the hypothesis of linear dependence of  $E_i$ ,  $i = 1, 2, 3$ , on  $x_3$ .

### 2.3 A Fully Coupled Nonlinear Model

We begin with a very general fully coupled model of a plate with surface mounted piezoelectric elements (see [9] and [10]). The inverse piezoelectric effect (i.e., the excitation of the electric field due to strains), electric properties of the surrounding substance (say air), and the quadratic terms in the strain tensor are taken into account.

Consider a plate with symmetrically mounted piezoelectric elements.

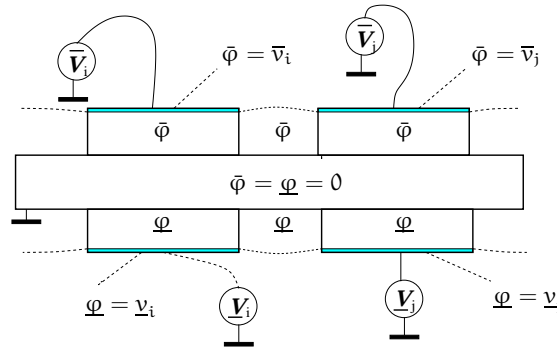


**Figure 2.** Fragment of a plate with many piezoelectric elements;  $\bar{\varphi}$  and  $\underline{\varphi}$  are potential functions,  $\bar{v}_i$  and  $\underline{v}_i$  are applied voltages

Let  $\Omega$  be the region of the plate;  $\Omega_{p_i}$  the projection of the  $i$ -th piezoelectric pair onto the middle plain of the plate;  $\Omega_p = \bigcup_i \Omega_{p_i}$ ;  $\Omega_s = \Omega \setminus \Omega_p$ ;  $u_1$  and  $u_2$  longitudinal displacements of points laying on the middle plain;  $w$  the transversal deflection;  $\bar{v}_i$  and  $\underline{v}_i$  voltages applied to the  $i$ -th piezoelectric pair;  $d$  the thickness of the substrate;  $h$  the thickness of the piezoelectric patches;  $\bar{E}_i = \partial \bar{\varphi} / \partial x_i$  and  $\underline{E}_i =$

$\partial \underline{\varphi} / \partial x_i$  the electric fields, where  $\bar{\varphi}$  and  $\underline{\varphi}$  are the potential functions. Assuming that  $\bar{E}_i$  and  $\underline{E}_i$  are linear in  $x_3$  and taking into account conventional boundary conditions for  $\bar{\varphi}$  and  $\underline{\varphi}$ , we can compute quadratic polynomials  $\bar{f}_1(x_3)$ ,  $\bar{f}_2(x_3)$ ,  $\underline{f}_1(x_3)$  and  $\underline{f}_2(x_3)$  such that the potentials within the  $i$ -th piezoelectric pair are given by

$$\bar{\varphi}(x_1, x_2, x_3) = \bar{f}_1(x_3)\bar{v}_i + \bar{f}_2(x_3)\bar{\Phi}(x_1, x_2),$$

$$\underline{\varphi}(x_1, x_2, x_3) = \underline{f}_1(x_3)\underline{v}_i + \underline{f}_2(x_3)\underline{\Phi}(x_1, x_2),$$

where  $\bar{\Phi}(x_1, x_2)$  and  $\underline{\Phi}(x_1, x_2)$  are unknown distributions of the electric field above and below the plate along the  $\{x_1, x_2\}$ -plane.

Using relations (1), (2), (3) and Kirchhoff-Love-Koiter hypothesis (6) yields the energy density within the piezoelectric patches and the substrate:

$$\begin{aligned} \bar{\chi}^p &= \frac{1}{2}c_{\alpha\beta\gamma\mu}^p s_{\alpha\beta} s_{\gamma\mu} + \frac{1}{2}x_3^2 c_{\alpha\beta\gamma\mu}^p w_{x_\alpha x_\beta} w_{x_\gamma x_\mu} - e_{i\alpha\beta} s_{\alpha\beta} \bar{E}_i \\ &\quad - \frac{1}{2}\epsilon_{ij} \bar{E}_i \bar{E}_j + x_3 c_{\alpha\beta\gamma\mu}^p s_{\alpha\beta} w_{x_\gamma x_\mu} - x_3 e_{i\alpha\beta} w_{x_\alpha x_\beta} \bar{E}_i; \end{aligned}$$

$$\begin{aligned} \underline{\chi}^p &= \frac{1}{2}c_{\alpha\beta\gamma\mu}^p s_{\alpha\beta} s_{\gamma\mu} + \frac{1}{2}x_3^2 c_{\alpha\beta\gamma\mu}^p w_{x_\alpha x_\beta} w_{x_\gamma x_\mu} - e_{i\alpha\beta} s_{\alpha\beta} \underline{E}_i \\ &\quad - \frac{1}{2}\epsilon_{ij} \underline{E}_i \underline{E}_j + x_3 c_{\alpha\beta\gamma\mu}^p s_{\alpha\beta} w_{x_\gamma x_\mu} - x_3 e_{i\alpha\beta} w_{x_\alpha x_\beta} \underline{E}_i; \end{aligned}$$

$$\chi^s = \frac{1}{2}c_{\alpha\beta\gamma\mu}^s s_{\alpha\beta} s_{\gamma\mu} + \frac{1}{2}x_3^2 c_{\alpha\beta\gamma\mu}^s w_{x_\alpha x_\beta} w_{x_\gamma x_\mu} + x_3 c_{\alpha\beta\gamma\mu}^s s_{\alpha\beta} w_{x_\gamma x_\mu};$$

$$\begin{aligned} F &= \int \int_{\Omega_p} \int_{d/2}^{d/2+h} \bar{\chi}^p dx_3 + \int \int_{\Omega_p} \int_{-d/2-h}^{-d/2} \underline{\chi}^p dx_3 + \int \int_{\Omega} \int_{-d/2}^{d/2} \chi^s dx_3 \\ &\quad + \int \int_{\Omega_s} \int_{d/2}^{d/2+h} \epsilon_0 \bar{E}_i^2 dx_3 + \int \int_{\Omega_s} \int_{-d/2-h}^{-d/2} \epsilon_0 \underline{E}_i^2 dx_3. \end{aligned}$$

Here,  $\epsilon_0$  is the material dielectric constant of the air, while

$$c_{\alpha\beta\gamma\mu}^s = C'_{\alpha\beta\gamma\mu} - \frac{C'_{33\alpha\beta} C'_{33\gamma\mu}}{C'_{3333}}$$

with  $C'$  being the elastic stiffness tensor of the substrate. Moreover,

$$\begin{aligned} c_{\alpha\beta\gamma\mu}^p &:= C_{\alpha\beta\gamma\mu} - \frac{C_{33\alpha\beta} C_{33\gamma\mu}}{C_{3333}}, \quad e_{i\alpha\beta} := e_{i\alpha\beta} - \frac{C_{33\alpha\beta} e_{i33}}{C_{3333}}, \\ \epsilon_{ij} &:= \epsilon_{ij} + \frac{e_{i33} e_{j33}}{C_{3333}}, \end{aligned}$$

where  $C$ ,  $e$  and  $\epsilon$  are the elastic stiffness tensor, piezoelectric stress tensor and material dielectric tensor involved in (1). Note that the old notations for  $e$  and  $\epsilon$  are kept. The in-plane strain tensor is given by

$$s_{\alpha\beta} = 1/2(u_{\alpha x_\beta} + u_{\beta x_\alpha} + w_{x_\alpha} \cdot w_{x_\beta}). \quad (8)$$

The application of the variational principle [7] leads to the equations

$$\begin{aligned} & \rho w_{tt} + \frac{\partial}{\partial x_\beta} (\sigma_{\alpha\beta} w_{x_\alpha}) + \Delta(\gamma \Delta w) - \theta \frac{\partial}{\partial x_\beta} (e_{\gamma\alpha\beta} w_{x_\alpha} (\bar{\phi}_{x_\gamma} + \underline{\phi}_{x_\gamma})) + \\ & \theta \frac{\partial^2}{\partial x_\alpha \partial x_\beta} (e_{3\alpha\beta} (\bar{\phi} + \underline{\phi})) - r \frac{\partial^2}{\partial x_\alpha \partial x_\beta} (e_{\gamma\alpha\beta} (\bar{\phi}_{x_\gamma} - \underline{\phi}_{x_\gamma})) - \\ & q \frac{\partial}{\partial x_\beta} (e_{3\alpha\beta} w_{x_\alpha} (\bar{v} - \underline{v})) - \ell \frac{\partial^2}{\partial x_\alpha \partial x_\beta} (e_{3\alpha\beta} (\bar{v} + \underline{v})) = 0; \\ & \rho u_{\alpha tt} - \frac{\partial}{\partial x_\beta} \sigma_{\alpha\beta} + \theta \frac{\partial}{\partial x_\beta} (e_{\gamma\alpha\beta} (\bar{\phi}_{x_\gamma} + \underline{\phi}_{x_\gamma})) + \\ & q \frac{\partial}{\partial x_\beta} e_{3\alpha\beta} (\bar{v} - \underline{v}) = 0, \quad \alpha = 1, 2; \\ & a \frac{\partial}{\partial x_\alpha} (\epsilon_{\alpha\beta} \bar{\phi}_{x_\beta}) + b \epsilon_{33} \bar{\phi} + \theta \frac{\partial}{\partial x_\gamma} (e_{\gamma\alpha\beta} s_{\alpha\beta}) + \\ & r \frac{\partial}{\partial x_\gamma} e_{\gamma\alpha\beta} w_{x_\alpha x_\beta} - \theta \frac{\partial}{\partial x_\alpha} e_{3\alpha\beta} w_{x_\beta} - g \epsilon_{33} \bar{v} = 0; \\ & a \frac{\partial}{\partial x_\alpha} (\epsilon_{\alpha\beta} \underline{\phi}_{x_\beta}) + b \epsilon_{33} \underline{\phi} + \theta \frac{\partial}{\partial x_\gamma} (e_{\gamma\alpha\beta} s_{\alpha\beta}) - \\ & r \frac{\partial}{\partial x_\gamma} e_{\gamma\alpha\beta} w_{x_\alpha x_\beta} - \theta \frac{\partial}{\partial x_\alpha} e_{3\alpha\beta} w_{x_\beta} - g \epsilon_{33} \underline{v} = 0; \end{aligned}$$

where

$$\sigma_{\alpha\beta} = \frac{1}{2} \ell_{\alpha\beta\mu\nu} (u_{\mu x_\nu} + u_{\nu x_\mu} + w_{x_\mu} w_{x_\nu}) \quad (9)$$

is the in-plane stress tensor;  $\rho$ ,  $\gamma$ ,  $e_{i\alpha\beta}$ ,  $\epsilon_{\alpha\beta}$  and  $\ell_{\alpha\beta\mu\nu}$  are piecewise constant discontinuous functions with jumps on the boundary of  $\Omega_p$ .

The constants  $a$ ,  $b$ ,  $\theta$ ,  $r$ ,  $\ell$ ,  $q$ ,  $g$  are computed from the problem's data. Moreover,

$$\underline{v} = \sum \underline{v}_i(t) I_{\Omega_{p_i}}(x_1, x_2), \quad \bar{v} = \sum \bar{v}_i(t) I_{\Omega_{p_i}}(x_1, x_2),$$

where  $I_{\Omega_{p_i}}$  is the indicator function of  $\Omega_{p_i}$ . Introduce the notation:

$$\vec{u} = (u_1, u_2, w), \quad \vec{\phi} = (\bar{\phi}, \underline{\phi}), \quad \vec{v} = (\bar{v}, \underline{v}),$$

$$H = (L_2(\Omega))^3, \quad V = (H_0^1(\Omega))^2 \times H_0^2(\Omega), \quad \Phi = (H^1(\Omega))^2.$$

**Theorem 1 (Solvability: see [9, 10]).**

*If  $\vec{u}(0) \in V$ ,  $\vec{u}_t(0) \in H$  and  $\vec{v} \in H^1(0, T; \mathbb{R}^2)$ , then the system has a solution such that:*

$$\vec{u} \in L_\infty(0, T; V), \quad \vec{u}_t \in L_\infty(0, T; H), \quad \vec{\phi} \in L_\infty(0, T; \Phi). \quad \square$$

The uniqueness can also be proved, if some additional smoothness of solutions is assumed. Such an assumption is not realistic since the smoothness can not be improved because of discontinuity of the coefficients.

## 2.4 Simplified Models

### *Electrically Decoupled Nonlinear Models*

Nonlinear models without the inverse piezoelectric effect involve coupled equations for the transversal and longitudinal displacements, whereas the equations for the electric field vanish because the electric field is defined immediately through the applied voltages (see (7)). It was assumed that piezoelectric and substrate materials are nearly isotropic, and voltages on the lower piezoelectric patches are equal to zero. These assumptions lead to the equations:

$$\begin{aligned} \rho w_{tt} - \Delta(\gamma \Delta w) - \frac{\partial}{\partial x_\alpha} (\sigma_{\alpha\beta} w_{x_\beta}) = \\ K \Delta(v_i(t) I_{\Omega_{p_i}}) + G \frac{\partial}{\partial x_\alpha} (w_{x_\alpha} v_i(t) I_{\Omega_{p_i}}), \quad (10) \\ \rho u_{\alpha tt} - \frac{\partial}{\partial x_\beta} \sigma_{\alpha\beta} = G \frac{\partial}{\partial x_\alpha} (v_i(t) I_{\Omega_{p_i}}), \quad \alpha = 1, 2. \end{aligned}$$

Here  $\Delta$  is the Laplace operator;  $K$  and  $G$  are constants;  $\rho$  and  $\gamma$  are piecewise constant discontinuous functions with jumps on the boundary of  $\Omega_p$ ;  $v_i(t)$  is a voltage applied to the  $i$ -th piezoelectric element.

The solvability follows from the previous theorem (see also [11]) but the uniqueness is not proved because of the discontinuous coefficients that violate the regularity of solutions.

### *Linear Models*

The simplest mathematical model is related to the case, where the nonlinear terms in (6) and the inverse piezoelectric effect, the second equation of (1), are omitted. The equation for  $w$  is independent from  $u_1, u_2$  and given by

$$\rho(x_1, x_2) w_{tt} + \Delta(\gamma(x_1, x_2) \Delta w) = K \Delta(v_i(t) \cdot I_{\Omega_{p_i}}(x_1, x_2)). \quad (11)$$

Note that discontinuous coefficients and unbounded input operators are inherent even in this simple model. Taking into account the inverse piezoelectric effect yields electrically coupled linear models that involve additional equations for  $u_1, u_2$  and the electric field (see, e.g., [13]). The linear case is good from the mathematical point of view because the corresponding equations are uniquely solvable and solutions are differentiable with respect to model parameters (see [12] and [13]).

## 2.5 Shells with Piezoelectric Actuators

The theory of usual thin shells is summarized very good in [8]. Consider a shell with two piezoelectric patches mounted symmetrically with respect to the middle surface. Let  $(\xi^1, \xi^2) \in \Omega$  be curvilinear coordinates of the middle surface of the shell;  $\Omega_p$  the region of the piezoelectric pair;  $\Omega_s = \Omega \setminus \Omega_p$  the region of the uncovered substrate;  $\xi^3$  the transversal coordinate along the normal;  $r$  the radius-vector of shell points;  $a$  the metric tensor of the middle surface;  $b$  the curvature tensor of the

middle surface;  $g$  the global metric tensor related to the shell coordinate system;  $u_1, u_2$  and  $u_3$  displacements of points of the middle surface;  $d$  the thickness of the substrate;  $h$  the thickness of the piezoelectric patches;  $v_1(t)$  and  $v_2(t)$  voltages applied to the piezoelectric patches. Let the vertical bar before a subscript denotes the corresponding covariant derivative. The strain tensor of the middle surface is given by the formula

$$\gamma_{\alpha\beta}(\vec{u}) = 1/2(u_{\alpha|\beta} + u_{\beta|\alpha}) - b_{\alpha\beta}u_3.$$

In the case of the Koiter model, where the conservation of the normal is assumed, the curvature change is given by

$$\varrho_{\alpha\beta}(\vec{u}) = -(u_{3|\alpha\beta} - b_{\alpha}^{\lambda}b_{\lambda\beta}u_3 + b_{\alpha|\beta}^{\lambda}u_{\lambda} + b_{\alpha}^{\lambda}u_{\lambda|\beta} + b_{\beta}^{\lambda}u_{\lambda|\alpha}).$$

The strain tensor is of the form

$$\begin{aligned}\varepsilon_{\alpha\beta}(\vec{U}) &= \gamma_{\alpha\beta}(\vec{u}) + \xi^3 \varrho_{\alpha\beta}(\vec{u}) \\ \varepsilon_{3\alpha}(\vec{U}) &= 0 \\ \varepsilon_{33}(\vec{U}) &= -\frac{\nu}{1-\nu} a^{\alpha\beta} \varepsilon_{\alpha\beta}(\vec{U}).\end{aligned}$$

The variation of the energy is given by the formula

$$\begin{aligned}a^K[\vec{u}, \vec{\varphi}; v_1, v_2] &= \\ &\int_{\Omega} d\sqrt{a} E^{\alpha\beta\lambda\mu} \left[ \gamma_{\alpha\beta}(\vec{u}) \gamma_{\lambda\mu}(\vec{\varphi}) + \frac{d^2}{12} \varrho_{\alpha\beta}(\vec{u}) \varrho_{\lambda\mu}(\vec{\varphi}) \right] d\xi^1 d\xi^2 + \\ &\int_{\Omega_p} \sqrt{a} \left\{ \frac{v_1(t)}{h} \int_{d/2}^{d/2+h} e^{3k1} \varepsilon_{kl}(\vec{\varphi}) d\xi^3 + \frac{v_2(t)}{h} \int_{-d/2-h}^{-d/2} e^{3k1} \varepsilon_{kl}(\vec{\varphi}) d\xi^3 \right\} d\xi^1 d\xi^2.\end{aligned}\quad (12)$$

The bilinear form  $a^K$  is defined on the space

$$\vec{V}^K(\Omega) = \{ \vec{u} : u_1, u_2 \in H^1(\Omega); u_3 \in H^2(\Omega); \vec{u}|_{\Gamma_0} = \partial u_3 / \partial n|_{\Gamma_0} = 0 \}.$$

The coefficients  $E^{\alpha\beta\lambda\mu}$  are discontinuous functions of  $\xi^1$  and  $\xi^2$ . In the case of shells with actuators made of piezoelectric ceramics belonging to the hexagonal class (6m m), the coefficients are of the form

$$E^{\alpha\beta\lambda\mu} = \begin{cases} E_s^{\alpha\beta\lambda\mu}(\xi^1, \xi^2), & (\xi^1, \xi^2) \in \Omega_s; \\ E_p^{\alpha\beta\lambda\mu}(\xi^1, \xi^2), & (\xi^1, \xi^2) \in \Omega_p; \end{cases} \quad \nu = \begin{cases} \nu_s, & (\xi^1, \xi^2) \in \Omega_s; \\ \nu_p, & (\xi^1, \xi^2) \in \Omega_p; \end{cases}$$

$$E_s^{\alpha\beta\lambda\mu} = \frac{E_s}{2(1+\nu_s)} \left( a^{\alpha\lambda} a^{\beta\mu} + a^{\alpha\mu} a^{\beta\lambda} + \frac{2\nu_s}{1-2\nu_s} a^{\alpha\beta} a^{\lambda\mu} \right),$$

$$E_p^{\alpha\beta\lambda\mu} = \frac{\hat{E}_p}{2(1 + \hat{\nu}_p)} \left( a^{\alpha\lambda} a^{\beta\mu} + a^{\alpha\mu} a^{\beta\lambda} + \frac{2\hat{\nu}_p}{1 - 2\hat{\nu}_s} a^{\alpha\beta} a^{\lambda\mu} \right),$$

$$\hat{E}_p = x + xy/(x + y), \quad \hat{\nu}_p = y/(x + y),$$

$$x = \frac{d}{(2h + d)} \frac{E_s}{1 + \nu_s} + \frac{2h}{2h + d} \frac{E_p}{1 + \nu_p},$$

$$y = \frac{d}{2h + d} \frac{\nu_s E_s}{1 + \nu_s} + \frac{2h}{2h + d} \frac{\nu_p E_p}{1 + \nu_p},$$

$$e^{fhs}(\xi^1, \xi^2, \xi^3) = g^{fi} g^{hj} g^{sk} e_{mnl}^{00} \frac{\partial r^m}{\partial \xi^i} \frac{\partial r^n}{\partial \xi^j} \frac{\partial r^l}{\partial \xi^k}.$$

The subscripts  $s$  and  $p$  point out to substrate and piezoelectric materials, respectively. The symbols  $\nu_s, \nu_p, E_s, E_p$  and  $e_{mnl}^{00}$  denote the Poisson ratios, Young moduli and piezoelectric stress tensor in the Euclidean coordinate system, while  $\hat{\nu}_p$  and  $\hat{E}_p$  denote the effective Poisson ratio and Young module of the substrate-piezoelectric structure. It is convenient to introduce the following seven parameters

$$\begin{aligned} p_1 &= \frac{E_s}{1 + \nu_s}, & p_2 &= \frac{E_s \nu_s}{(1 + \nu_s)(1 - 2\nu_s)}, \\ p_3 &= \frac{\hat{E}_p}{1 + \hat{\nu}_p}, & p_4 &= \frac{\hat{E}_p \hat{\nu}_p}{(1 + \hat{\nu}_p)(1 - 2\hat{\nu}_p)}, \\ p_5 &= e_{311}^{00}, & p_6 &= e_{333}^{00}, & p_7 &= e_{113}^{00} \end{aligned}$$

that define all of the coefficients. Besides, the form  $a^K$  is linear in  $\vec{p} = (p_1, \dots, p_7)$ .

According to the variational principle, the dynamic equations are given by

$$\int_{\Omega} \sqrt{\alpha} \rho \bar{u}_{tt} \bar{\varphi} d\xi^1 d\xi^2 + a^K[\bar{u}, \bar{\varphi}; \nu_1, \nu_2] = 0, \quad \bar{\varphi} \in \vec{V}^K(\Omega). \quad (13)$$

The initial and boundary conditions look like that

$$\bar{u}|_{t=0} = \bar{u}^0, \quad \bar{u}_t|_{t=0} = \bar{u}^{0'}, \quad \bar{u}|_{\Gamma_0} = 0, \quad \partial u_3 / \partial n|_{\Gamma_0} = 0.$$

The following theorem states the existence and the uniqueness of solutions for models of the Koiter's type. The proof follows from the properties of the elliptic part, the first integral, of (12) stated in [8]. The input operator, the second integral, is similar to that in [11].

**Theorem 2.** *If  $\bar{u}^0 \in \vec{V}^K(\Omega)$ ,  $\bar{u}^{0'} \in (L_2(\Omega))^3$ ,  $\nu_1(\cdot), \nu_2(\cdot) \in H^1(0, T)$ , then the system (13) is uniquely solvable. The solution  $\bar{u}$  possesses the regularity:*

$$\bar{u} \in C([0, T]; \vec{V}^K(\Omega)), \quad \bar{u}_t \in C([0, T]; (L_2(\Omega))^3). \quad \square$$

### 3 IDENTIFICATION OF PARAMETERS FOR SHELLS

We propose two procedures appropriate for the treatment of composite structures. The first one is related to the minimization of a residual of dynamic equations (see [14]). The second procedure is the conventional least squares method supported by the “strong” differentiability of solutions with respect to parameters (see [12]).

#### 3.1 Minimization of Residual

A solution  $\vec{u}$  is measured at few points that lie sufficiently dense in a subset  $\Omega_m$  of  $\Omega$  so that they form a triangulation of  $\Omega_m$ . Then, an approximation  $\vec{u}^\varepsilon$  of the solution and its derivatives is computed from the measured data using Finite Elements. Here  $\varepsilon$  denotes the error due to the approximation and measurement. The residual on the region  $\Omega_m$  is a functional that is equal to zero on the exact solution and positive for other functions. We use the following form of the residuum:

$$\ell(\vec{u}^\varepsilon, \vec{\psi}, \vec{p}) = \int_{\Omega_m} \sqrt{\alpha} \rho \vec{u}_{tt}^\varepsilon \vec{\psi} d\xi^1 d\xi^2 + \alpha_m^K[\vec{u}^\varepsilon, \vec{\psi}; \vec{p}], \quad \vec{\psi} \in \vec{V}^K(\Omega),$$

where  $\alpha_m^K$  is defined in the same way that  $\alpha^K$  but with the integration over  $\Omega_m$  instead of  $\Omega$ . The dependence of  $\alpha_m^K$  on  $\vec{p}$  is indicated, whereas the dependence on  $v_1$  and  $v_2$  is omitted. Let  $\Pi$  be a set that a priori bounds the exact parameter vector  $\vec{p}$ . An approximation  $\vec{p}^\varepsilon$  is being found as the minimizer of the functional  $\ell$ , that is

$$\vec{p}^\varepsilon = \arg \min_{\vec{p} \in \Pi} \int_0^T \ell(\vec{u}^\varepsilon, \vec{\psi}^{t, \vec{p}, \varepsilon}, \vec{p}) dt, \quad (14)$$

where the auxiliary function  $\vec{\psi}^{t, \vec{p}, \varepsilon}$  satisfies the equation

$$(\vec{\psi}^{t, \vec{p}, \varepsilon}, \omega)_{\vec{V}_\varepsilon^K} = \ell(\vec{u}^\varepsilon, \vec{\omega}, \vec{p}), \quad \forall \vec{\omega} \in \vec{V}_\varepsilon^K, \quad t \in [0, T].$$

Here,  $\vec{V}_\varepsilon^K$  is a finite element approximation of the space  $\vec{V}^K(\Omega)$ . Because of the linearity of both  $\ell(\vec{u}^\varepsilon, \vec{\psi}, \vec{p})$  and  $\vec{\psi}^{t, \vec{p}, \varepsilon}$  with respect to  $\vec{p}$ , the integral in (14) is a quadratic form, i.e.

$$\int_0^T \ell(\vec{u}^\varepsilon, \vec{\psi}^{t, \vec{p}, \varepsilon}, \vec{p}) dt = \vec{p}' Q_\varepsilon \vec{p} - 2q'_\varepsilon \vec{p} + d_\varepsilon =: G_{\Omega_m}^\varepsilon(\vec{p}). \quad (15)$$

The matrix  $Q_\varepsilon$  has the following structure:

$$Q_\varepsilon = \int_0^T R'_\varepsilon(t) D_\varepsilon^{-1} R_\varepsilon(t) dt, \quad (16)$$

where  $R_\varepsilon$  is some matrix and  $D_\varepsilon^{-1}$  is a positive definite matrix.

**Proposition 3 (see [14]).** *If solutions of (13) possess the following additional regularity:  $\int_0^T \|\vec{u}_{tt}\|_{L_2(\Omega_m)}^2 \leq \infty$ , then the approximation  $\vec{u}^\varepsilon$  can be chosen such that  $\int_0^T \left( \|\vec{u}_{tt}^\varepsilon - \vec{u}_{tt}\|_{L_2(\Omega_m)}^2 + \|\vec{u}^\varepsilon - \vec{u}\|_{V^\kappa(\Omega_m)}^2 \right) dt \rightarrow 0$  as  $\varepsilon \rightarrow 0$ .*

**Proposition 4. (see [14])** *Let  $\Pi^0$  be the set of the parameters that are compatible with the exact solution. There is a function  $Z(\varepsilon)$  such that  $Z(\varepsilon) \rightarrow 0$  as  $\varepsilon \rightarrow 0$ , and*

$$\sup_{\vec{p} \in \Pi^0} |G_{\Omega_m}^\varepsilon(\vec{p}) - G_{\Omega_m}^\varepsilon(\vec{p}^\varepsilon)| \leq Z(\varepsilon). \quad \square$$

We assume in addition that  $\Omega_m$  depends on  $\varepsilon$  and may shrink with  $\varepsilon$ . Suppose that the function  $G_{\Omega_m}^\varepsilon(\vec{p})$  defined by (15) has the following properties:

- G1. There is a unique minimizing element  $\vec{p}^\varepsilon \in \Pi$  of the function  $G_{\Omega_m}^\varepsilon(\cdot)$ .
- G2. There is  $\nu > 0$  and a positive function  $X(\Omega_m, \varepsilon)$  such that, for any  $\vec{p} \in \Pi$ ,

$$G_{\Omega_m}^\varepsilon(\vec{p}) - G_{\Omega_m}^\varepsilon(\vec{p}^\varepsilon) \geq X(\Omega_m, \varepsilon) \|\vec{p} - \vec{p}^\varepsilon\|^\nu.$$

**Theorem 5 (see [14]).** *If  $Z(\varepsilon)/X(\Omega_m, \varepsilon) \rightarrow 0$  as  $\varepsilon \rightarrow 0$ , then the set of all parameters compatible with the exact solution consists of a unique element  $\vec{p}^0$ , and  $\vec{p}^\varepsilon \rightarrow \vec{p}^0$  as  $\varepsilon \rightarrow 0$ .*

*Remark 6.* Properties G1 and G2 express the positive definiteness of the matrix  $Q_\varepsilon$  (this matrix depends on the domain  $\Omega_m$ ). As a rule, the function  $X$  decreases with  $\Omega_m$  and is almost insensitive w.r.t.  $\varepsilon$ . Therefore, if  $\Omega_m$  decreases not too quick with  $\varepsilon$ , the conditions of the Theorem are expected to be satisfied. Note that the matrix under the integral in (16) is positive semi-definite for each  $t$ . The resulting matrix  $Q_\varepsilon$  has a good chance to be positive definite and well conditioned, if the zero spaces of  $R'_\varepsilon(t)D_\varepsilon^{-1}R_\varepsilon(t)$  vary with  $t$ . This corresponds to the accumulation of the information during the observation.

### 3.2 Last Squares Method

The formal differentiation of (13) w.r.t. the parameters yields the so-called variational equations

$$\int_{\Omega} \sqrt{\alpha} \rho \vec{u}_{j\,tt} \vec{\varphi} + \alpha^K [\vec{u}_j, \vec{\varphi}; \vec{p}] + \alpha^K [\vec{u}, \vec{\varphi}; \vec{l}_j] = 0. \quad (17)$$

Here, the following notation is used:

$$\vec{u}_j = \partial \vec{u} / \partial p_j, \quad \vec{l}_j = (0, \dots, \overset{j}{1}, \dots, 0).$$

**Theorem 7 (see [12]).** *Let  $\vec{u}^0 = 0$ ,  $\vec{u}^{0'} = 0$ ,  $v_\alpha(\cdot) \in H^3(0, T)$ ,  $v_\alpha(0) = 0$ ,  $v'_\alpha(0) = 0$ ,  $\alpha = 1, 2$ . Then the solution  $\vec{u}$  of (13) is continuously differentiable w.r.t.  $\vec{p}$ . The partial derivatives can be computed from the variational equations (17).  $\square$*

The parameters fitting can be done using a gradient descent method, where the gradient is computed using (17). Moreover, higher derivatives exist and can be computed using a sequence of variational equations similar to (17). This makes possible the application of SQP methods.

### 3.3 Simulation

To illustrate theoretical results, consider a cylindric shell with a piezoelectric pair as in Figure 3.

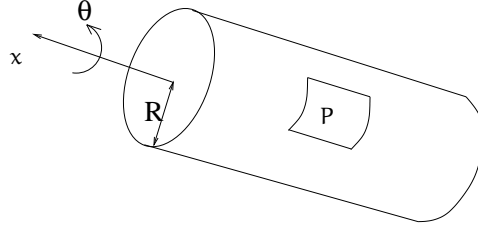


**Figure 3.** Cylindric shell;  $s = x/R$  and  $\theta$  is the polar angle

The coordinates of the middle surface are defined through the variable  $s = x/R$  and the polar angle  $\theta$ .

The equations read:

$$\begin{aligned} \rho u_{1tt} + (a u_{1s} + b u_{2\theta} + b u_3)_s + (c u_{2s} + c u_{1\theta})_\theta &= m(t)K(I_{\Omega_p})_\theta, \\ \rho u_{2tt} + (b u_{1s} + a u_{2\theta} + a u_3)_\theta + (c u_{2s} + c u_{1\theta})_s &= m(t)K(I_{\Omega_p})_\theta + n(t)G(I_{\Omega_p})_\theta, \\ \rho u_{3tt} + b u_{1s} + a u_{2\theta} + a u_3 + \Delta(k \Delta u_3) &= n(t)G \Delta I_{\Omega_p} - n(t)G - m(t)K. \end{aligned}$$

Here, the notation is used:

$$m(t) = v_1(t) + v_2(t), \quad n(t) = v_1(t) - v_2(t).$$

The coefficients  $\rho$ ,  $a$ ,  $b$ ,  $c$ ,  $k$  are of the form:

$$\begin{aligned} \rho(s, \theta) &= \rho_p I_{\Omega_p} + (1 - I_{\Omega_p}) \rho_s, & a(s, \theta) &= a_p I_{\Omega_p} + (1 - I_{\Omega_p}) a_s, \\ b(s, \theta) &= b_p I_{\Omega_p} + (1 - I_{\Omega_p}) b_s, & c(s, \theta) &= c_p I_{\Omega_p} + (1 - I_{\Omega_p}) c_s, \\ k(s, \theta) &= k_p I_{\Omega_p} + (1 - I_{\Omega_p}) k_s, \end{aligned}$$

Assume that  $\rho_s$  and  $\rho_p$  are known parameters because they can be easily measured. Thus, the parameters  $a_p$ ,  $b_p$ ,  $c_p$ ,  $k_p$ ,  $a_s$ ,  $b_s$ ,  $c_s$ ,  $k_s$ ,  $K$ ,  $G$  are to estimate.

*Results*

Here, the process of estimation based on the differentiability of solution w.r.t. parameters is shown. The transversal deflection is measured at 20 spatial points for 100 times with the error equal to 5%. The least squares problem is solved using a gradient descent method. The gradient is computed from the corresponding variational equations. In Figure 4, the horizontal axes represent the number of steps of the gradient descent method.

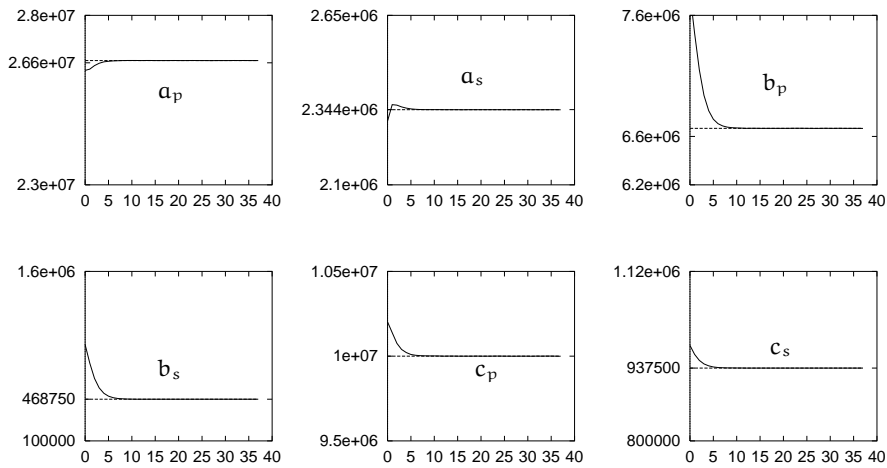


**Figure 4.** Estimations of several parameters. Error is equal to 5%

4 HOMOGENIZATION

Consider a von Kármán plate with surface mounted numerous piezoelectric actuators that form a self similar periodic structure (see Figure 5).

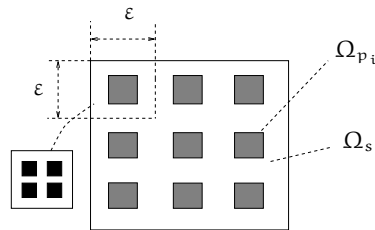


**Figure 5.** Self similar structure. Refinement of each cell if  $\epsilon := \epsilon/2$

The inverse piezoelectric effect and the interaction with the surrounding substance are omitted but the geometrical nonlinearities are accounted. The dynamic equations can be written (compare with 10) as follows.

PROBLEM  $P_\varepsilon$ .

$$\rho\left(\frac{x}{\varepsilon}\right) w_{tt}^\varepsilon - \operatorname{div}\left(\mu\left(\frac{x}{\varepsilon}\right) \nabla w_{tt}^\varepsilon\right) + \Delta\left(\gamma\left(\frac{x}{\varepsilon}\right) \Delta w^\varepsilon\right) - \frac{\partial}{\partial x_\alpha}\left(\sigma_{\alpha\beta}^\varepsilon w_{x_\beta}^\varepsilon\right) = \\ \mathbf{K}\Delta\left(V(t, x)I\left(\frac{x}{\varepsilon}\right)\right) + G\frac{\partial}{\partial x_\alpha}\left(w_{x_\alpha}^\varepsilon V(t, x)I\left(\frac{x}{\varepsilon}\right)\right).$$

$$\rho\left(\frac{x}{\varepsilon}\right) u_{\alpha tt}^\varepsilon - \frac{\partial}{\partial x_\beta}\sigma_{\alpha\beta}^\varepsilon = G\frac{\partial}{\partial x_\alpha}\left(V(t, x)I\left(\frac{x}{\varepsilon}\right)\right), \quad \alpha = 1, 2.$$

Here,  $\sigma_{\alpha\beta}^\varepsilon = \ell_{\alpha\beta\lambda\eta}\left(\frac{x}{\varepsilon}\right)\left(u_{\lambda x_\eta}^\varepsilon + u_{\eta x_\lambda}^\varepsilon + w_{x_\lambda}^\varepsilon w_{x_\eta}^\varepsilon\right)$  is the in-plane stress tensor,  $\ell_{\alpha\beta\lambda\eta}$ ,  $\rho$ ,  $\mu$ ,  $\gamma$ ,  $I$  are  $1 \times 1$ -periodic piecewise-constant discontinuous functions,  $V(t, x)$  is a distributed applied voltage. The inertia of mechanical moments is taken into account through the term  $\operatorname{div}\left(\mu\left(\frac{x}{\varepsilon}\right) \nabla w_{tt}^\varepsilon\right)$ . The boundary and initial conditions are imposed,

$$w|_{\partial\Omega} = 0, \quad \frac{\partial w}{\partial \vec{n}}\Big|_{\partial\Omega} = 0, \quad w|_{t=0} = w_0, \quad w_t|_{t=0} = w'_0, \quad (18) \\ u_\alpha|_{\partial\Omega} = 0, \quad u_\alpha|_{t=0} = u_{\alpha 0}, \quad u_{\alpha t}|_{t=0} = u'_{\alpha 0}.$$

A homogenization procedure based on two-scale convergence (see [15] and [16]) yields the following limiting equations with constant coefficients.

PROBLEM  $P$ .

$$\hat{\rho}w_{tt} - \hat{\mu}\Delta w_{tt} + \hat{\gamma}\Delta^2 w - \frac{\partial}{\partial x_\alpha}\left(\hat{\sigma}_{\alpha\beta} w_{x_\beta}\right) \\ = \mathbf{K}\hat{I}\Delta V(t, x) + G\hat{J}_{\alpha\beta}\frac{\partial}{\partial x_\alpha}\left(w_{x_\beta} V(t, x)\right), \\ \hat{\rho}u_{\alpha tt} - \frac{\partial}{\partial x_\beta}\hat{\sigma}_{\alpha\beta} = G\hat{J}_{\alpha\beta}\frac{\partial}{\partial x_\beta}V(t, x), \quad \alpha = 1, 2.$$

The stress tensor contains only constant coefficients:

$$\hat{\sigma}_{\alpha\beta} = \hat{\ell}_{\alpha\beta\lambda\eta}\left(u_{\lambda x_\eta} + u_{\eta x_\lambda} + w_{x_\lambda} w_{x_\eta}\right).$$

Boundary and initial values are the same, see (18). The coefficients are given by

$$\hat{\rho} = \langle \rho(y) \rangle, \quad \hat{\mu} = \langle \mu(y) \rangle, \quad \hat{\gamma} = \langle 1/\gamma(y) \rangle^{-1}, \quad \hat{I} = -\langle 1/\gamma(y) \rangle^{-1} \langle I(y)/\gamma(y) \rangle,$$

$$\hat{\ell}_{\alpha\beta\lambda\eta} = \left\langle \ell_{\alpha\beta\tau\theta}(y) \left( \delta_{\tau\lambda} \delta_{\theta\eta} + \frac{\partial N_{\tau\lambda\eta}(y)}{\partial y_\theta} + \frac{\partial N_{\theta\lambda\eta}(y)}{\partial y_\tau} \right) \right\rangle, \\ \hat{J}_{\alpha\beta} = \left\langle \ell_{\alpha\beta\tau\theta}(y) \left( \frac{\partial M_\tau(y)}{\partial y_\theta} + \frac{\partial M_\theta(y)}{\partial y_\tau} \right) + \delta_{\alpha\beta} I(y) \right\rangle.$$

The auxiliary functions  $N_{1\lambda\eta}(\mathbf{y})$ ,  $N_{2\lambda\eta}(\mathbf{y})$ ,  $(\lambda, \eta) = (1, 1), (2, 2), (1, 2), (2, 1)$ ,  $M_1(\mathbf{y})$ , and  $M_2(\mathbf{y})$  are defined by elliptic systems which are to be solved on the unit square  $[0, 1] \times [0, 1]$ .

$$\begin{cases} \frac{\partial}{\partial y_\beta} \left[ \ell_{\mu\nu 1\beta}(\mathbf{y}) \left( \delta_{\mu m} \delta_{\nu n} + \frac{\partial N_{\mu\lambda\eta}}{\partial y_\nu} + \frac{\partial N_{\nu\lambda\eta}}{\partial y_\mu} \right) \right] = 0, \\ \frac{\partial}{\partial y_\beta} \left[ \ell_{\mu\nu 2\beta}(\mathbf{y}) \left( \delta_{\mu m} \delta_{\nu n} + \frac{\partial N_{\mu\lambda\eta}}{\partial y_\nu} + \frac{\partial N_{\nu\lambda\eta}}{\partial y_\mu} \right) \right] = 0. \\ \frac{\partial}{\partial y_\beta} \left[ \ell_{\mu\nu 1\beta}(\mathbf{y}) \left( \frac{\partial M_\mu}{\partial y_\nu} + \frac{\partial M_\nu}{\partial y_\mu} \right) + \delta_{1\beta} I(\mathbf{y}) \right] = 0, \\ \frac{\partial}{\partial y_\beta} \left[ \ell_{\mu\nu 2\beta}(\mathbf{y}) \left( \frac{\partial M_\mu}{\partial y_\nu} + \frac{\partial M_\nu}{\partial y_\mu} \right) + \delta_{2\beta} I(\mathbf{y}) \right] = 0. \end{cases}$$

The boundary conditions must be  $[0, 1] \times [0, 1]$ -periodic, which yields the solvability and the uniqueness up to a constant.

The following theorem (see [17]) states the relation between problems  $\mathbf{P}_\varepsilon$  and  $\mathbf{P}$ .

**Theorem 8.** *If  $w_0 = 0$ ,  $w'_0 = 0$ ,  $u_{\alpha 0} = 0$ ,  $u'_{\alpha 0} = 0$ ,  $V \in H^2(0, T; L_2(\Omega))$ ,  $V(0, \cdot) = 0$ , then problem  $\mathbf{P}$  has a unique strong solution  $(w, u_\alpha)$  that possesses the following regularity:*

$$\begin{aligned} w &\in C([0, T]; H^2_0(\Omega)) \cap C^1([0, T]; H^1_0(\Omega)) \cap \\ &W^2_\infty(0, T; H^1_0(\Omega)) \cap L_\infty(0, T; H^3(\Omega)). \\ u_\alpha &\in C([0, T]; H^1_0(\Omega)) \cap C^1([0, T]; L_2(\Omega)) \cap \\ &W^2_\infty(0, T; L_2(\Omega)) \cap L_\infty(0, T; H^2(\Omega)). \end{aligned}$$

The set  $G_\varepsilon$  of all limits of Galerkin approximations of  $\mathbf{P}_\varepsilon$  shrinks to  $(w, u_\alpha)$  as  $\varepsilon \rightarrow 0$ , that is all sequences  $(w^\varepsilon, u_\alpha^\varepsilon) \in G_\varepsilon$  converge to  $(w, u_\alpha)$  in

$$C^1([0, T]; H^2_0(\Omega)) \times C^1([0, T]; H^1_0(\Omega))$$

as  $\varepsilon \rightarrow 0$ . □

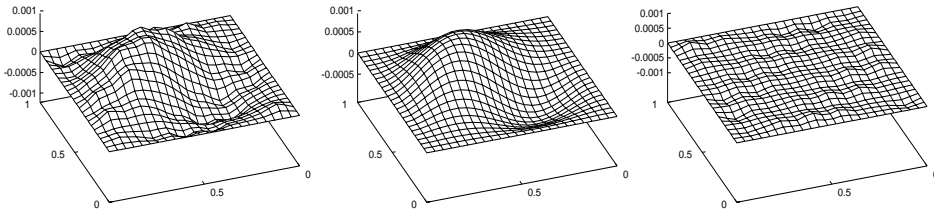


**Figure 6.** Snapshot of solutions to  $\mathbf{P}_\varepsilon$  and  $\mathbf{P}$  and their difference. The number of uniformly distributed piezoelectric actuators is equal to 36

In conclusion of this subsection, we note that the general fully coupled system can also be homogenized. Nevertheless, the result obtained in [10] is weaker than the claim of the previous theorem: the relation between the original and limiting equations is very weak so that the  $L_2$ -convergence holds for  $u_\alpha^\varepsilon$ , and the  $H^1$ -convergence holds for  $w^\varepsilon$ . Another feature consists in arising new nonlinear terms in the limiting equations. This leads to the idea to control the creations of such terms to improve the structure of the limiting equations with respect to their controllability and observability.

## 5 USING HOMOGENIZATION FOR CONTROL DESIGN

For brevity, consider the control design for equation (11). Assume that the number of piezoelectric actuators is controlled by the refinement parameter  $\varepsilon$  (see Figure 6). Then, the equation reads

$$\rho w_{tt}^\varepsilon + \Delta(\gamma \Delta w^\varepsilon) = K \Delta \left( \sum_{i=1}^{n_p(\varepsilon)} v_i(t) \cdot I_{\Omega_{p_i}} \right). \quad (19)$$

We begin with a distributed voltage  $V \in H^1(0, T; L_2(\Omega))$  that defines voltages applied to the piezoelectric actuators as follows:

$$v_i(t) = \frac{1}{\text{meas}(\Omega_{p_i})} \int_{\Omega_{p_i}} V(t, x) dx, \quad i = 1, \dots, n_p(\varepsilon). \quad (20)$$

The voltages  $v_i(t)$ ,  $i = 1, \dots, n_p(\varepsilon)$ , define the function

$$V^\varepsilon(t, x) = \begin{cases} V(t, x), & x \in \Omega_s, \\ \text{meas}(\Omega_{p_i})^{-1} \int_{\Omega_{p_i}} V(t, x) dx, & x \in \Omega_{p_i}. \end{cases}$$

$V^\varepsilon$  is constant on each piezoelectric actuator and approximates the distributed control  $V$ . Now, we can rewrite equation (19) as follows

$$r\left(\frac{x}{\varepsilon}\right) w_{tt}^\varepsilon + \Delta\left(g\left(\frac{x}{\varepsilon}\right) \Delta w^\varepsilon\right) = K \Delta\left(V^\varepsilon I\left(\frac{x}{\varepsilon}\right)\right), \quad (21)$$

where  $r(y)$ ,  $g(y)$ , and  $I(y)$  are appropriate  $1 \times 1$  periodic functions. The homogenization procedure yields a limiting equation of the form

$$\hat{r} w_{tt} + \hat{g} \Delta^2 w = K \hat{I} \Delta V. \quad (22)$$

One can prove that  $w^\varepsilon \rightarrow w$ , in  $C([0, T]; \mathcal{E}^{0, \nu}(\bar{\Omega}))$ ,  $\nu < 1$ , where  $\mathcal{E}^{0, \nu}(\bar{\Omega}) \subset C(\bar{\Omega})$  is the Hölder space. Using the notation,  $v(t, x) = K \hat{I} \Delta V(t, x)$ , we rewrite (22) as follows

$$\hat{r} w_{tt} + \hat{g} \Delta^2 w = v(t, x). \quad (23)$$

Note that (23) does not contain unbounded operators on the right-hand-side. Let  $v(t, x)$  be the optimal control for (23), then the optimal control for (22) is the solution of the Laplace equation

$$\Delta V = (\hat{K}\hat{I})^{-1} v(t, x), \quad V|_{\partial\Omega} = 0. \quad (24)$$

**Theorem 9.** *Let  $v(t, x)$  be the optimal control in (23), and  $v_i(t)$ ,  $i = 1, \dots, m_p$ , are defined through (24) and (20). Then*

$$\lim_{\varepsilon \rightarrow 0} \|w^\varepsilon - w\|_{C([0, T]; \mathcal{E}^{0, \nu}(\bar{\Omega}))} = 0,$$

where  $w^\varepsilon$  and  $w$  are solutions of (19) and (23), respectively.  $\square$

The proof follows from the fact that  $V^\varepsilon \rightarrow V$  in  $H(0, T; L_2(\Omega))$  and from the results of [17] about the convergence rate of  $w^\varepsilon$  to a limiting solution.

## 6 STABILIZATION OF SHELLS WITH PIEZOELECTRIC ACTUATORS

A method for stabilizations of shells is described in [18]. An auxiliary open-loop control problem is stated and the dependence of the adjoint variable on the initial state vector of the shell equations is computed.

For a shell with two symmetrically mounted piezoelectric patches, the variation (12) of the total energy is of the form

$$\alpha^K[\bar{u}, \bar{\varphi}; v_1(t), v_2(t)] = \alpha_0^K[\bar{u}, \bar{\varphi}] + \vec{v}(t) \cdot \vec{L}[\bar{\varphi}],$$

with  $\vec{v} = (v_1, v_2)$  and  $\vec{L} = (L_1, L_2)$ , where  $L_1$  and  $L_2$  are clearly to obtain from (12). This representation holds in the case of several pairs of actuators, if the appropriate dimension of the vectors  $\vec{v}$  and  $\vec{L}$  is meant. The auxiliary functional is defined as follows:

$$J_T = \frac{\ell}{2} \int_{\Omega} |\bar{u}(T)|^2 d\xi_1 d\xi_2 + \frac{b}{2} \int_{\Omega} |\bar{u}_t(T)|^2 d\xi_1 d\xi_2 + \frac{c}{2} \int_0^T |\vec{v}(t)|^2 dt.$$

The coupled system of the shell and adjoint equations reads:

$$\int_{\Omega} \sqrt{\alpha} \rho \bar{u}_{tt} \bar{\varphi} d\xi^1 d\xi^2 + \alpha_0^K[\bar{u}, \bar{\varphi}] = -c^{-1} \vec{L}^K[\bar{\pi}] \cdot \vec{L}^K[\bar{\varphi}], \quad \forall \bar{\varphi} \in \vec{V}^K(\Omega),$$

$$\int_{\Omega} \sqrt{\alpha} \rho \bar{\pi}_{tt} \bar{\psi} d\xi^1 d\xi^2 + \alpha_0^K[\bar{\pi}, \bar{\psi}] = 0, \quad \forall \bar{\psi} \in \vec{V}^K(\Omega),$$

$$\begin{aligned} \bar{u}(0) &= \bar{u}^0, & \bar{u}_t(0) &= \bar{u}^{0'}, \\ \bar{\pi}(T) &= b \bar{u}_t(T), & \bar{\pi}_t(T) &= -\ell \bar{u}(T). \end{aligned}$$

The optimal control  $\vec{v}_T^0$  of the auxiliary problem is defined through the adjoint variable as follows

$$\vec{v}_T^0(t; \vec{u}^0, \vec{u}^{0'}) = c^{-1} \vec{L}^K[\vec{\pi}].$$

An approximation of the optimal stabilizing control is given by the formula

$$\vec{v}_{\text{stb}}(\vec{u}^0, \vec{u}^{0'}) = \vec{v}_T^0(0; \vec{u}^0, \vec{u}^{0'}). \quad (25)$$

*Proof (Sketch of the proof).* The following representation holds

$$\vec{v}_T(t; \vec{u}^0, \vec{u}^{0'}) = c^{-1} \mathcal{B} \mathcal{P}(t, T) \begin{pmatrix} \vec{u}(t; \vec{u}^0, \vec{u}^{0'}) \\ \vec{u}_t(t; \vec{u}^0, \vec{u}^{0'}) \end{pmatrix},$$

where the input operator  $\mathcal{B}$  is defined by the relation:  $\mathcal{B}\vec{\pi} = \vec{L}^K[\vec{\pi}]$  for all  $\vec{\pi} \in \vec{V}^K(\Omega)$ , while  $\mathcal{P}(t, T)$  is the solution of the corresponding operator Riccati equation (see, e.g., [6]). According to (25), we obtain

$$\vec{v}_{\text{stb}}(\vec{u}^0, \vec{u}^{0'}) = c^{-1} \mathcal{B} \mathcal{P}(0, T) \begin{pmatrix} \vec{u}^0 \\ \vec{u}^{0'} \end{pmatrix}.$$

It is known that the optimal stabilizing control is defined by

$$\vec{v}_{\text{opt}}(\vec{u}^0, \vec{u}^{0'}) = c^{-1} \mathcal{B} \mathcal{P} \begin{pmatrix} \vec{u}^0 \\ \vec{u}^{0'} \end{pmatrix},$$

where  $\mathcal{P}$  is a solution of the corresponding stationary Riccati equation. Moreover,  $\mathcal{P}(0, T) \rightarrow \mathcal{P}$  as  $T \rightarrow \infty$ . Thus,  $\vec{v}_{\text{stb}}(\vec{u}^0, \vec{u}^{0'})$  approximates  $\vec{v}_{\text{opt}}(\vec{u}^0, \vec{u}^{0'})$  and, therefore, stabilizes the system, whenever  $T$  is sufficiently large.

## 7 ACTIVE SOUND REDUCTION

The control design that we want to discuss in this section differs from that discussed in Section 6 because the control actions must be computed in real-time from some incomplete information about the state of the object. This information is the history of the signal measured on sensors up to the current time. This section is closely related to the investigation [2] and [19].

### 7.1 Physical Model

The physical model is a container with a sound source within them. The problem consists in the reduction of the sound that is radiated by the structure. The control circuit includes piezoelectric actuators and sensors delivering information about the current state (see Figure 7).

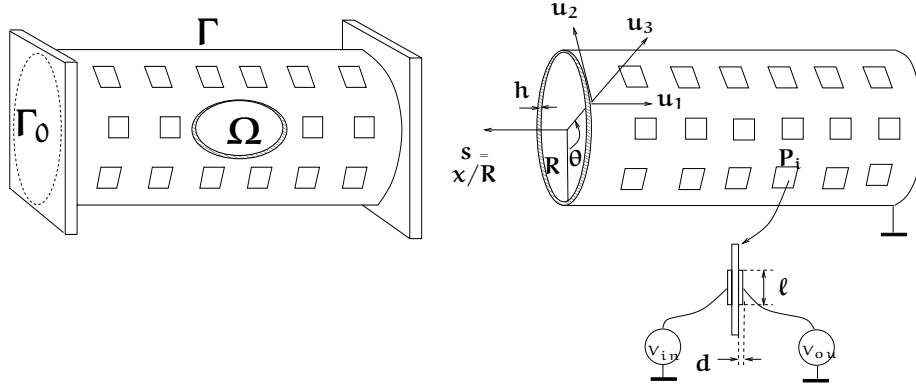


Figure 7. Physical Model

### 7.2 Coupled Acoustic Structure

This system describes the interface between acoustic waves and a cylindrical shell

$$\phi_{tt} = c^2 \Delta \phi \quad \text{on } \Omega,$$

$$\nabla \phi \vec{n}|_{\Gamma_0} = 0, \quad \phi_r|_{\Gamma} = u_{3t}.$$

$$\rho u_{1tt} + (a u_{1s} + b u_{2\theta} + b u_3)_s + (c u_{2s} + c u_{1\theta})_\theta = K v_i(t) (I_{p_i})_s,$$

$$\rho u_{2tt} + (b u_{1s} + a u_{2\theta} + a u_3)_\theta + (c u_{2s} + c u_{1\theta})_s = L v_i(t) (I_{p_i})_\theta, \quad (\theta, s) \in \Gamma,$$

$$\rho u_{3tt} + b u_{1s} + a u_{2\theta} + a u_3 + \Delta k \Delta u_3 = G v_i(t) \Delta I_{p_i} - \hat{\rho} \phi_t(t, R, \theta, s).$$

Boundary conditions read:  $u_1 = u_2 = u_3 = u_{3s} = 0$  on  $\Gamma_0$ ;  $u_1, u_2, u_3$  are periodic in  $\theta$ . Here,  $\phi$  is the acoustic potential;  $u_i, i = 1, 2, 3$ , are the tangential and transversal displacements;  $\theta$  is the polar angle;  $s = x/R$  is the specific length. The coefficients  $a, b, c, k$  are of the form:  $a(s, \theta) = a_{piez} I_p + a_{sub} s (1 - I_p)$ , where  $I_p$  is the indicator function of the region related to the piezoelectric actuators.

### 7.3 Reduced Basis Method and Proper Orthogonal Decomposition

First, the coupled acoustic system is approximated very carefully to obtain a sufficient number of "snapshots" of the solution or its time derivatives at various times:

$$y_j(\theta, s) = \begin{pmatrix} u_1(t_j, \theta, s) \\ u_2(t_j, \theta, s) \\ u_3(t_j, \theta, s) \end{pmatrix} \quad \text{or} \quad y_j(\theta, s) = \begin{pmatrix} u_{1t}(t_j, \theta, s) \\ u_{2t}(t_j, \theta, s) \\ u_{3t}(t_j, \theta, s) \end{pmatrix}, \quad j = 1, \dots, N_s$$

where  $u_k(t, \theta, s)$ ,  $k = 1, 2, 3$ , is a solution of the coupled elastic-acoustic system. Then, the covariation matrix,

$$C_{kl} = \frac{1}{N_s} \langle y_k, y_l \rangle,$$

is computed along with the eigenvalues and eigenvectors,

$$\lambda_1 \geq \lambda_2 \geq \dots \lambda_{N_s} \geq 0; \quad \alpha^1, \alpha^2, \dots, \alpha^{N_s}; \quad \alpha^k \cdot \alpha^l = \begin{cases} 0, & k \neq l \\ 1/(\lambda_k N_s), & k = l. \end{cases}$$

New basis functions  $\Phi_j$ ,  $j = 1, \dots, N_r$ , are chosen in such a way:

$$\Phi_j = \sum_{i=1}^{N_s} \alpha_i^j y_i, \quad j = 1, \dots, N_r \ll N_s, \quad (N_s \approx 100, \quad N_r \approx 3 \div 6).$$

Thus, the reduced basis yields a low dimensional Galerkin approximation,

$$\dot{x}(t) = A x(t) + B V_{\text{inp}}(t) + g(t), \quad V_{\text{out}}(t) = C x(t), \quad x \in \mathbb{R}^{2N_r}, \quad (26)$$

of the coupled acoustic system. Here,  $N_r$  is the dimension of the reduced basis;  $V_{\text{inp}}$  and  $V_{\text{out}}$  are the vectors of applied and measured voltages on the piezoelectric actuators and sensors, respectively;  $g(t)$  is an unpredictable disturbance due to the acoustic excitation.

It is known from  $H^\infty$  theory that the feedback control is given by the relation

$$V_{\text{inp}}(t) = -K x_c(t),$$

where  $x_c(t)$  is the solution of the so called compensator equation,

$$\begin{aligned} \dot{x}_c(t) &= A_c x_c(t) - F V_{\text{out}}(t), \\ A_c &= A - FC - BK + \gamma^{-2} \hat{Q} \Pi, \\ K &= R^{-1} B' \Pi, \quad F = [I - \gamma^{-2} \hat{\Pi} \Pi]^{-1} \hat{\Pi} C' \hat{R}^{-1}. \end{aligned}$$

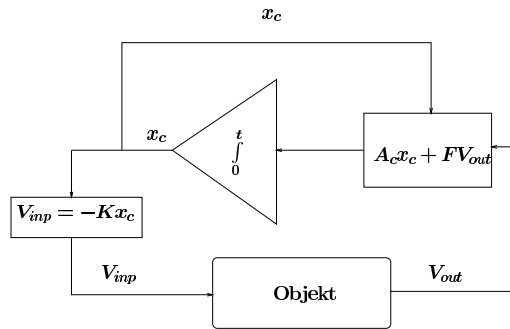
Here, the matrices  $\Pi$  and  $\hat{\Pi}$  satisfy two Riccati equations,

$$\begin{aligned} \Pi A + A' \Pi - \Pi [B R^{-1} B' - \gamma^{-2} \hat{Q}] \Pi + Q &= 0, \\ \hat{\Pi} A' + A \hat{\Pi} - \hat{\Pi} [B \hat{R}^{-1} B' - \gamma^{-2} Q] \hat{\Pi} + \hat{Q} &= 0, \end{aligned}$$

related to (26) and to a quadratic functional of the form

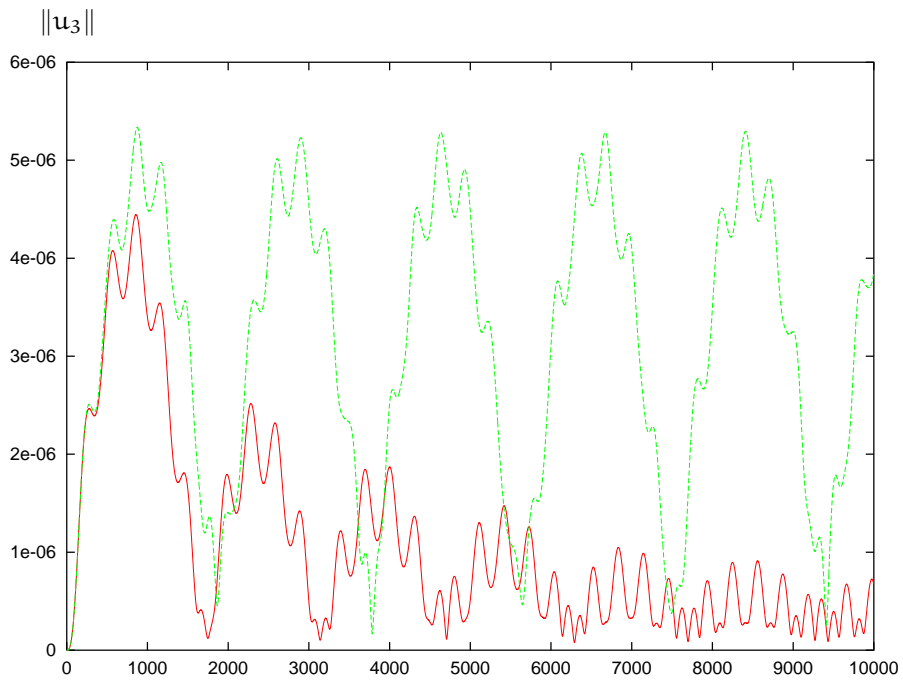
$$J = \int_0^\infty \{ \langle Q x, x \rangle + \langle R V_{\text{inp}}, V_{\text{inp}} \rangle - \gamma^2 |g(t)|^2 \} dt. \quad (27)$$

Thus, the control circuit is implemented as follows:



7.4 Results of the Simulation

The dotted curve denotes a free multi-frequency oscillation. The solid curve represents damped oscillations. The duration is equal to 0.001 s. The number of actuators and sensors is equal to 36



### 7.5 Another Auxiliary Functional

The utilization of other auxiliary functionals for the feed-back control design in (26) is possible and, maybe, preferable. For example, the functional

$$J = \int_0^{\infty} \left\{ \sqrt{\langle Qx, x \rangle} + \langle R V_{\text{inp}}, V_{\text{inp}} \rangle - \gamma^2 |g(t)|^2 \right\} dt \quad (28)$$

provides a slower growth with respect to the state vector than (27). This guarantees the existence of the value function of the control problem independently from the disturbance  $g$  in (26) even though the observation contains arbitrary large disturbances. The computation of the value function is based on some stochastic procedures (see [20] and [21]). Nevertheless the final formulae are pure deterministic and can be implemented numerically. Roughly speaking, the optimal control at the state  $x(t)$  and subject to the measured signal  $\{V_{\text{out}}(\tau), 0 \leq \tau \leq t\}$  is computed through the solution of the problem

$$h^0 \rightarrow \min_{|h|=1} \{ \langle \mathcal{D}h, h \rangle - \langle x(t), h \rangle \},$$

where  $\mathcal{D}$  is a positive semidefinite matrix that is easily computed using the problem data and the signal  $\{V_{\text{out}}(\tau), 0 \leq \tau \leq t\}$ .

### REFERENCES

1. A. Preumont, *Vibration Control of Active Structures*. Solid Mechanics and its Applications. **50**, Kluwer Academic Publisher (Dordrecht-Boston-London) 1997.
2. H. T. Banks, R. C. Smith and Y. Wang, *Smart material structures: modeling, estimation and control*. Wiley, Chichester 1996.
3. J. Zelenka, *Piezoelectric Resonators and their Applications*. Studies in Electrical and Electronic Engineering. **24**, Elsevier 1986.
4. G. A. Maugin, *Continuum mechanics of electromagnetic solids*. North-Holland series in Applied Mathematics and mechanics. **33**, North-Holland 1987.
5. T. Basar and P. Bernhard, *H<sup>∞</sup>-Optimal Control and Related Minimax Design Problems*. Birkhäuser, Boston 1987.
6. I. Lasiecka and R. Triggiani, *Control theory for partial equations: continuous and approximation theories. II. Abstract hyperbolic-like systems over a finite time horizon*. Encyclopedia of mathematics and its applications **75**, Edited by G.-C.Rota, Cambridge University Press 2000.
7. L. D. Landau and E. M. Lifschitz, *Elastizitätstheorie*. Akademie-Verlag (Berlin) 1975.
8. M. Bernadou, *Finite Element Methods for Thin Shell Problems*. Wiley (Chichester) 1996.
9. K.-H. Hoffmann and N. D. Botkin, *A Fully coupled model of a nonlinear thin plate excited by piezoelectric actuators*. Smart materials. Proceedings of the first caesarium, Bonn, Nov. 17–19, 1999. Edited by K.-H. Hoffmann, Springer 2001, available on the preprint server<sup>1</sup>.
10. K.-H. Hoffmann and N. D. Botkin, *Homogenization of a fully coupled model of a nonlinear thin plate excited by piezoelectric actuators*. International conference: Optimal

<sup>1</sup> <http://www.zib.de/dfg-echtzeit/Publikationen/index.html>

- Control of Complex Structures, Mathematical Research Center Oberwolfach, June, 4–10, 2000 (to appear in proceedings, available on the preprint server<sup>2</sup>).
11. K.-H. Hoffmann and N. D. Botkin, *Oscillations of nonlinear thin plates excited by piezoelectric patches*, ZAMM: Z. angew. Math. Mech., **78** (1998), 495–503.
  12. N. D. Botkin, *Estimation of parameters of a linear thin plate*. Analysis **17** (1997) 367–378.
  13. N. D. Botkin, W. G. Litvinov, Y. I. Rubezhansky, *Models and problems for piezoelectric elastic bodies and thin shells*. DFG-Project "Echtzeit-Optimierung großer Systeme", Preprint 99-5. Preprintserver<sup>3</sup>
  14. N. D. Botkin, *Estimation of parameters of thin plates excited by piezoelectric patches*. Preprint of the Technical University of Munich. M9704, 1997.
  15. G. Allaire, *Homogenization and two-scale Convergence*, SIAM J. Math. Anal., **23** (6) (1992), 1482–1518.
  16. H. Haller, *Verbundwerkstoffe mit Formgedächtnislegierung – Mikromechanische Modellierung und Homogenisierung*, Dissertation, TU-München 1997.
  17. K.-H. Hoffmann and N. D. Botkin, *Homogenization of von Kármán plates excited by piezoelectric patches*, ZAMM: Z. angew. Math. Mech., **133** (1999), 191–200.
  18. K.-H. Hoffmann and N. D. Botkin, *Adaptive Materialien in der Echtzeitoptimierung*. DFG-Projekt "Echtzeitoptimierung großer Systeme", Arbeitsbericht über den ersten Förderungszeitraum von 1995–1997. München 1997 (available on the preprint server<sup>4</sup>).
  19. H. T. Banks, R. C. H. Rosario and R. C. Smith, *Reduced order model feedback control design: computational studies for thin cylindrical shells*. Report of the Center for Research in Scientific Computation. North Carolina State University. CRSC-TR98-24, June, 1998.
  20. N. N. Krasovskii, *Control for dynamic system (in Russian)*. Nauka (Moscow), 1985.
  21. N. N. Krasovskii, *Control problems with incomplete information (in Russian)*. Academy of Sciences of USSR, Ural Scientific Center, Institute of Mathematics and Mechanics (Sverdlovsk) 1984.

---

<sup>2</sup> <http://www.zib.de/dfg-echtzeit/Publikationen/index.html>

<sup>3</sup> <http://www.zib.de/dfg-echtzeit/Publikationen/index.html>

<sup>4</sup> <http://www.zib.de/dfg-echtzeit/Publikationen/index.html> as Project report. I.